Journal of Polymer Research (2021) 28:313
https://doi.org/10.1007/s10965-021-02646-3

ORIGINAL PAPER

Role of free volume in mechanical behaviors of side chain lcp grafted products of high density polyethylene

Behiye Ozturk Sen[1] · Sedat Cetin[2] · Ugur Yahşi[3] · Ugur Soykan[4]

Received: 23 March 2021 / Accepted: 1 July 2021

Abstract
The monomer, p-benzophenoneoxycarbonylphenyl methacrylate (BPOCPMA) the polymer of which exhibit mesomorphic behavior as side chain LCP has been graft copolymerized onto high density polyethylene (HDPE) in order to improve its properties. The PALS analysis of the products displayed that the graft copolymerization, while led to relatively small increase in the free volume size at low percentages of poly(BPOCPMA), resulted in decreases in the size and fraction of the free volume with the increase of poly(BPOCPMA) content. The graft copolymerization gave rise to remarkable improvements in the mechanical properties, especially in tensile strength and modulus, and the improvements were accompanied by the decreases in the free volume fraction. SEM analysis of the fracture surfaces of the mechanical test samples displayed a gradual transition from ductile fracture at low graft contents to brittle nature dominated at high percentages of poly(BPOCPMA). The XRD analysis showed significant expansions in the lateral dimensions (a and b parameters) of the orthorhombic unit cell in the crystalline domains of HDPE matrix, in consistence with poly(BPOCPMA) content. The grafting also gave rise to noteworthy increases in the crystalline melting temperature of the HDPE.

Keywords Grafting · Copolymers · Morphology · Free volume · Mechanical properties

Introduction

Polyethylene (PE) with the advantageous properties like light weight, high chemical resistance, relatively low cost and easy processability has widespread applications in many areas, from plastic pipes to containers and packaging film. In load performance applications, the concerns focus on the time-, temperature-, and strain-rate-dependent mechanical behaviors [1].

Liquid crystalline polymers (LCPs) are high strength and high modulus materials owing to high state of orientation and extension in their stiff molecular backbones. Because of their extraordinary mechanical characters, they have been combined with thermoplastics (TPs) in order to obtain materials with superior mechanical properties [2–8].

Mechanical performance of semicrystalline polymers under load is dependent on plastic deformation mechanism [9] as well as on the chemical structure, configuration, conformation and on microstructure [10–14]. The plastic deformation is a complicated process and involves changes in both amorphous and crystalline phases, however, the involvement varies with the stress applied [15–17]. In amorphous phase the macromolecules are relatively mobile at temperatures above the glass transition, and the phase has relatively low resistance to the deformation [18]. The entangled molecules and tie molecules in the phase form interlinks between the crystallities (lamellae). During stretching of the polymer the molecules transfer stresses, and therefore have a determining effect on the mechanical behaviors like fracture toughness [19–22]. When tensional load is applied to a polymer, initially the entropic elastic response occurs. The chain entanglements act like crosslinks [23], and the straining interlamellar macromolecules make elastic deformation almost entirely reversible. During the elastic deformation relatively minor deformation takes place

✉ Sedat Cetin
cetin_s@ibu.edu.tr

[1] Faculty of Pharmacy, Altınbas University, 34217 Bakırkoy, Istanbul, Turkey

[2] Department of Chemistry, Faculty of Arts and Sciences, Bolu Abant Izzet Baysal University, 14280 Bolu, Turkey

[3] Department of Physics, Faculty of Arts and Sciences, Marmara University, 34722 Goztepe, Istanbul, Turkey

[4] Yenicaga Yasar Celik Vocational High School, Bolu Abant Izzet Baysal University, 14300 Bolu, Turkey

Published online: 22 July 2021

in the lamellae that have stiffer nature. Due to the constraints imposed by the lamellae, on the other hand, a limited elastic deformation occur. With an increase of the load, the linearity in the load-strain dependence disappears [24], and plastic deformation of crystals accommodate the deformation of the material which involves molecular rearrangement of the chain-folded lamellar structure into chain unfolded fibrillar morphology. The deformation has been commonly identified to involve chain slip, transverse slip, deformation twinning, and a stress induced martensitic transformation [16, 17]. The slip mechanism, principally the dominant mode of plastic deformation, has a distinct importance since it can lead to much larger plastic strains comparing to the other mechanisms [17].

Many semicrystalline polymers exhibit cavitation (void formation) with size from nanometers to micrometers during tensile drawing inside amorphous phase between lamellae [25–32]. The onset of cavitation is usually observed around yield point [27–30], and lamellae fragmentation and cavitation are often detected simultaneously [31]. Its development was explained by the negative pressure arising between lamellae when they are separated by the applied stress [32]. The formation of cavities during crystallization of polymers was explained by Galeski [33], however, with polymer melt pockets locked by surrounding spherulites. Transformation of the melts to more dense crystals in the pockets give rise to the voids. Cavitation, on the other hand, plays an important role in the deformation of the material under load. The formation of the cavities results in a local release of stress around the voids [31, 33], triggering of the unravelling of the folded chains and thus breaking down the crystals [34], and leads to decrease in yield stress and yield strain [30]. Xiong et al. accept the formation of voids as one of the major antecedent processes leading to the fragmentation and fibrillar transformation of the crystalline lamellae beyond yielding [35]. On the role of free volume characteristics of polymer matrix in bulk physical properties of polymer nanocomposites, Sharma and Pujari [36] reported an inverse relation between the tensile properties of a polymer matrix and its free volume fraction. They explained the inverse relation by that the applied load is concentrated at the defect (free volume hole) which hampers the load distribution among the polymer molecules, leading to failure of the material. Hence, a polymer matrix having less free volume fraction would exhibit improved tensile properties. The inverse relation was also announced by Ponnamma et al. [37] in the study on free volume fraction and Young's modulus in natural rubber-MWCNTs composites. Therefore, it is crucial to take into account the voids to elucidate the mechanical behavior of probably all polymeric materials.

Positron annihilation lifetime spectroscopy (PALS) is one of the most important techniques to determine free volume, empty microscopic space that exists between molecules, and microstructural characterization in polymers [38]. The positively charged positrons reside and decay by forming positronium *(Ps),* which is intermediate state between positron and electron, in low electron density region [39]. According to free volume theories, ortho-positronium (*o-Ps)* particles exist in a free-volume region. The increment in the size of the void gives rise to lower positron sensitivity, however, higher ***Ps*** sensitivity in lower charge density region. Thus, it is suitable probe for the determination of free volume in polymers owing to *Ps* localization in the free volume holes in amorphous region [40, 41].

In this work, the effect of graft copolymerization of p-benzophenoneoxycarbonylphenyl methacrylate onto HDPE on the free volume properties of the material was studied in relation to the graft content, besides the effect on orthorhombic unit cell parameters (lateral dimensions) in crystalline domains of HDPE matrix. In addition, the mechanical behaviors of the products were investigated in relation to their free volume properties and the graft contents. The effect of the grafting on thermal and morphological properties of the material was also studied. For the products, it was presumed that the poly(BPOCPMA) chains in glassy nematic arrangement [42], with a high degree of long-range order, lead to increase in the orientation and alignment of HDPE chains in processing when constituted as grafted macromolecules. It was predicted that such developments in the structure would improve the properties of the material, especially its mechanical behaviors.

Experimental

Materials

The major chemicals used for the synthesis of the monomer BPOCPMA, methacryloyl chloride (Alfa Aesar A.G.), p-hydroxybenzoic acid (HBA), thionyl chloride (Merck A.G.), 4-hydroxybenzophenone (HBP) (Alfa Aesar A.G.), and dicumyl peroxide (DCP) (Merck A.G.) were used as received from the companies. All the other chemicals and solvents used in the preparation of the products were of analytical grade and used without any additional purification.

High density polyethylene (HDPE), a commercial product of Turkish Petrochemical Industry (PETKIM) and coded as S 0464, was used in the preparation of the products. The HDPE granules were dissolved in boiling xylene (138-139ºC) and precipitated by adding ethanol. The precipitate was filtered, dried in vacuum at 40ºC and ground after cooling in liquid nitrogen. The obtained HDPE powder was used in the graft copolymerization experiments.

BPOCPMA synthesis

The monomer, p-benzophenoneoxycarbonylphenyl methacrylate (BPOCPMA) was prepared in three steps. Firstly, p-methacryloyloxybenzoic acid (MBA) was produced by condensation reaction of p-hydroxybenzoic acid with methacryloyl chloride in alkaline medium as reported by Sainath et. al [42]. Secondly, p-methacryloyloxybenzoyl chloride (MBC), used in the synthesis of the monomer, was prepared by refluxing the solution of p-methacryloyloxybenzoic acid (MBA) in thionyl chloride in the presence of a trace amount of dimethyl formamide for 7–8 h. Lastly, the monomer BPOCPMA was produced by stirring the equimolar solution of p-methacryloyloxybenzoyl chloride (MBC) and 4-hydroxybenzophenone in xylene containing pyridine for 3–4 days. The product BPOCPMA was purified by repeated recrystallizations from xylene, and characterized via DSC, ^{1}H-NMR and FT-IR techniques. White solid; 57% yield; melting point 130.1 ºC with respect to DSC; ^{1}H-NMR (400 MHz, DMSO-d_6, 25 ºC, TMS): δ (ppm) = 2.04 (3H, CH_3), 5.97–6.35 (2H, CH_2), 7.45–7.78 (4H, ArH), 7.53–7.88 (4H, ArH), 8.25–7.73–7.61 (5H, ArH). IR (KBr) ($\nu_{max,}$ cm^{-1}) 2990 (-CH_3), 1747 and 1736 (C = O), 1597 and 1504 (C = C), 1259 and 1198 (C–O–C), 974 and 927 (C-H out-of-plane).

Polymerization and graft copolymerization of BPOCPMA

Homopolymerization of BPOCPMA was carried out by bulk melt polymerization. The mixture of BPOCPMA and DCP (3% with respect to weight of the monomer) was heated at 140 °C in vacuum for 1 h. The product poly(BPOCPMA) was repeatedly washed with acetone and then with DMSO to remove residual monomer and byproducts, and dried in vacuum at 40 °C. The reaction yield was found to be 95%.

The graft copolymerization of BPOCPMA onto HDPE was also performed via bulk polymerization method. The reaction mixtures with varying compositions were prepared by mixing HDPE powder, BPOCPMA (5, 10, 15, 20, 30, 40% of the mixture) and DCP initiator (2% with respect to weight of BPOCPMA) in a mortar with extensive hand grinding. The mixtures were then heated up to 140 °C in vacuum and kept at this temperature for an hour. After being kept in DMSO for several hours, the products were extensively washed with DMSO again and then with acetone to remove residual monomer and byproducts, and dried in vacuum at 40 °C. These products were so called coproducts and comprised of both the poly(BPOCPMA) homopolymer and the poly(BPOCPMA)-g-PE graft copolymer macromolecules in the HDPE matrix. In order to remove poly(BPOCPMA) homopolymer from the products, some of the products agitated in hot DMF for several hours were washed with hot DMF again and then with acetone (the homopolymer was soluble in hot DMF) and thus to obtain the products so called copolymers involving only poly(BPOCPMA)-g-PE grafted macromolecules in the HDPE matrix.

Characterization

Fourier transform infrared (FTIR) spectra of the monomer, the intermediate products obtained in the monomer synthesis and of the grafted products were obtained with Shimadzu 8400 S FTIR spectrophotometer in the region of 400–4000 cm^{-1}. Bruker-Spectrospin Avance DPX 400 Ultra-shield ^{1}H-NMR spectrometer with a frequency of 400 MHz was used to determine ^{1}H-NMR spectrum of the monomer and of the intermediate products in dimethyl sulfoxide-d_6 and tetramethylsilane (TMS) was used as an internal reference. DSC analyses of the monomer and of the products were carried out with a Shimadzu DSC 60 Differential Scanning Calorimeter. All DSC runs were collected in the temperature range between 30 and 300ºC at a heating rate 10ºC/min. Crystalline characteristics of the products were studied by using a Rigaku Multiflex X-ray diffractometer with a Cu-Kα target giving a monochromatic beam (λ = 1.54 Å for Cu) at a scanning rate of 5º/min over the range of 2θ = 10º-60º and step increment of 0.02º in air at room temperature. Tensile behavior of the HDPE and the products were determined by a LLYOD LR5K Mechanical Tester with samples with gauge length of 50 mm, thickness of 2 mm, and width of 7.6 mm at room temperature. Crosshead speed in testing was 50 mm/min. The impact behavior of the samples prepared with dimensions of 1 mm (thickness) × 7 mm (width) were determined by Coesfeld Material Test Pendulum Impact Tester at room temperature. The results reported were an average of the results for test run on at least four samples. The test samples were prepared by injection molding at 220 °C with a Daca Instruments Microinjector with injection process at 8 bar. The morphologies of the tensile and impact fractured surfaces of the products were detected using JEOL 6390-LV scanning electron microscope with an accelerating voltage of 20 kV, and a resolution power of 3 nm. Prior to the analysis, all the fractured surfaces of the samples were coated with a thin layer of gold in order to improve the conductivity. Positron annihilation lifetime spectroscopy (PALS) was used in order to investigate free volume properties of neat HDPE and the products. PALS measurements were carried out at room temperature in Marmara Positronium Laboratory (MARPOS) in Physics Department at Marmara University. For this purpose, fast–fast conventional coincidence system has been employed measuring the elapsed time between the β^+ emission of ^{22}Na source, characterized by a 1.274 MeV photon as a birth signal of positron, and the annihilation

gamma emission of 0.511 MeV as a dead signal. The ^{22}Na source was prepared by depositing and evaporating about 20 μCi of ^{22}NaCI aqueous solution sandwiched between two pieces of sample with 0.5×0.5 cm^2 and 1 mm thickness. All lifetime spectra were resolved with the RESOLUTION and PATHFIT [43] programs to determine lifetimes and intensities with the system resolution, 528 ps (FWHM). 5 million counts were collected in each lifetime spectrum. The lifetimes of positrons for neat HDPE, copolymer and coproducts were determined and all lifetime spectra were resolved into three lifetime components, which are the shortest-lifetime component, T_1 and its intensity I_1 attributed to the annihilation of para-positronium (p-Ps), the intermediate component, T_1 and its intensity I_2, associated with the direct annihilation of positrons and the longest-lived component, τ_3 and its intensity I_3 attributed to pick off annihilation of ortho-positronium (o-Ps). These lifetime components were calculated using T_1 fixed at 125 ps, assumed as independent of free volume.

Results and discussions

Graft copolymerization

The graft copolymerization of BPOCPMA onto HDPE was successfully carried out, and the variation in the extent of grafting was investigated as a function of monomer concentration in reaction mixture. The free radicals arising in the reaction medium with heating brought about the formation of free radicals on both HDPE and vinylic group (functional group) of BPOCPMA. As a result of that, the graft copolymerization of BPOCPMA onto HDPE and homopolymerization reaction of BPOCPMA took place in the medium. Thus, content of poly(BPOCPMA) present as grafted chains in the copolymers and as both grafted and homopolymer macromolecules in the coproducts was determined gravimetrically. The results, the percentage of poly(BPOCPMA) in both classes of the products and percent grafting, were given in Table 1. Poly(BPOCPMA) content in the products increased consistently with BPOCPMA concentration in the reaction mixture. The maximum contents, 21.0% poly(BPOCPMA) in the copolymers and 26.7% poly(BPOCPMA) in the coproducts were obtained at 40% BPOCPMA. The percent grafting, on the other hand, reached a maximum of 75.3% at 15% BPOCPMA, which was followed by a dramatic decrease reducing to 49.1% grafting at 40% BPOCPMA. At lower monomer thus initiator (2% of weight of BPOCPMA) concentrations, radicals presumably formed on HDPE chains in majority due to the high probability of direct reactions between HDPE chains and the initiator radicals. Thus, the maximum grafting percentage was obtained at 15% BPOCPMA. On the other hand, the increase in the content of poly(BPOCPMA) as BPOCPMA concentration increased possibly due to the propagation of poly(BPOCPMA) macromolecules grafted onto HDPE chains, resulting in the formation of a high percentage of poly(BPOCPMA). In addition, it can also be stated that steric hindrance arising from the presence of the crowded groups on the BPOCPMA molecule may have increased the probability of radical formation on HDPE chains. This supports the proposed mechanism that the grafting took place via the radicals forming on HDPE chains rather than the reactions between propagating poly(BPOCPMA) radicals and HDPE chains.

On the other hand, the structural characterization of the neat HDPE, poly(BPOCPMA), the copolymer containing 6.7% of poly(BPOCPMA) and the coproduct with 26.7% of poly(BPOCPMA) was performed by means of FTIR analysis. The recorded spectra showing the characteristic absorption bands of the samples were depicted in Fig. 1. As regarding the spectrum of neat HDPE, the absorption bands of stretching vibrations of CH_2 group at 2920 and 2848 cm^{-1}, and the bands at 1558 and 1467 cm^{-1} due to the bending vibrations of the group. The band observed at 717 cm^{-1} was assigned to C–C bending vibrations. FTIR spectrum of the homopolymer poly(BPOCPMA) displayed a strong band at 1741 cm^{-1} due to C = O stretching vibrations of the ester groups. The absorption band ascribed to C = O stretching vibrations of benzophenone group was observed at 1658 cm^{-1}. The absorption bands due to C = C stretching vibrations of aromatic groups were recorded at 1599 and 1502 cm^{-1}. The bands at 1261 and 1201 cm^{-1} were attributed to C–O–C stretching vibrations. Therein, it was to be emphasized that the bands regarding vinylic C-H out-of-plane bending vibrations observed apparently at 927 and 974 cm^{-1} in the monomer spectrum were not detected in the spectrum of poly(BPOCPMA). This result verified that polymerization takes place over the vinylic group. As for the copolymer with 6.7% of poly(BPOCPMA) and the coproduct with 26.7% of poly(BPOCPMA), it was visible

Table 1 The variation of poly(BPOCPMA) content in the products with the monomer BPOCPMA percentage in the reaction mixture

% BPOCPMA in reaction mixture	5%	10%	15%	20%	30%	40%
% Poly(BPOCPMA) in the copolymers	3.8 ± 0.3	6.7 ± 0.7	10.7 ± 1.1	11.8 ± 0.4	18.6 ± 2.8	21.0 ± 0.6
% Poly(BPOCPMA) in the coproducts	3.8 ± 0.4	7.3 ± 0.8	12.7 ± 0.5	19.2 ± 0.9	25.1 ± 1.2	26.7 ± 1.3
% Grafting	69.4 ± 3.2	69.5 ± 6.8	75.3 ± 0.5	64.5 ± 0.6	51.3 ± 3.4	49.1 ± 9.6

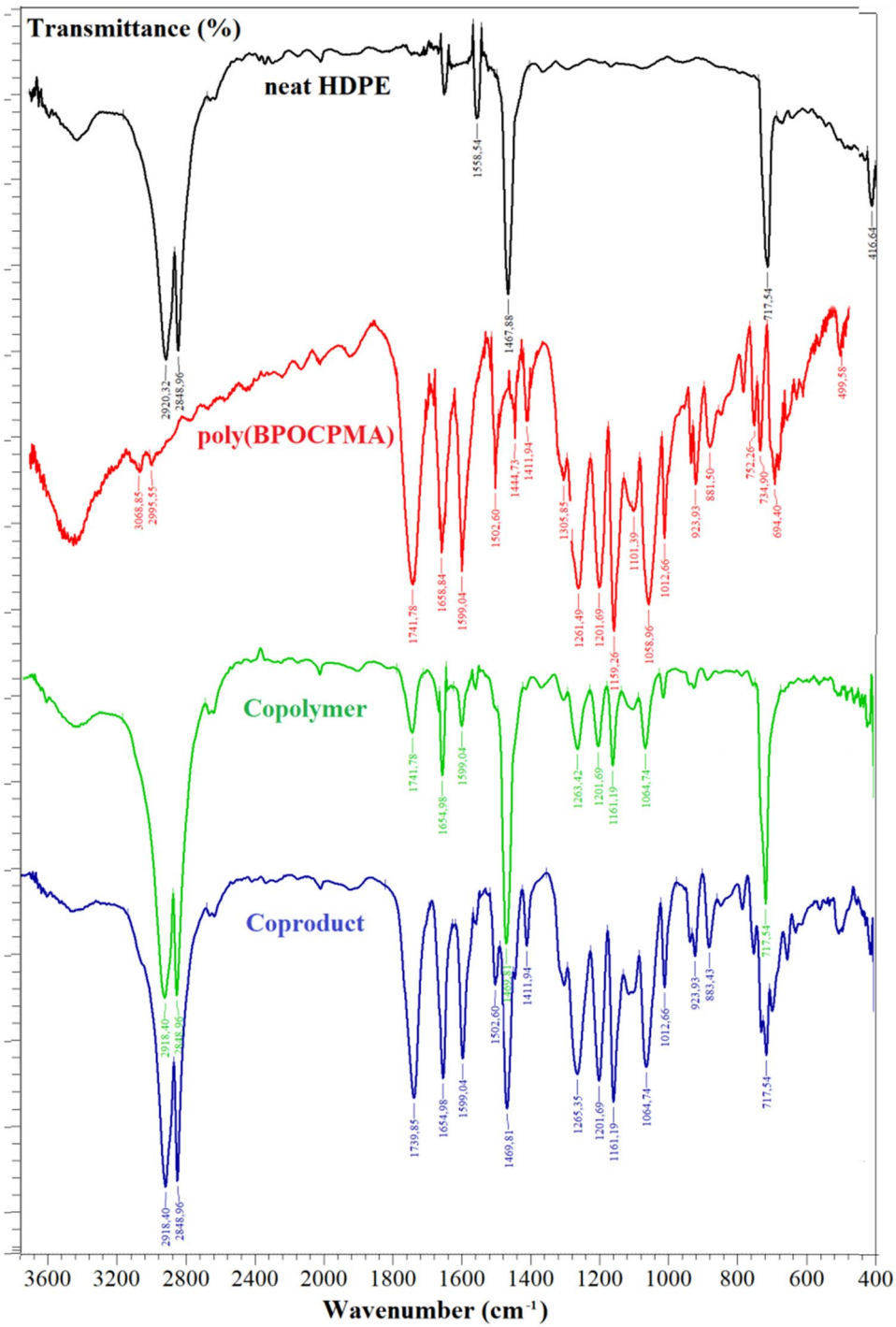

Fig. 1 FTIR spectrums of neat HDPE, poly(BPOCPMA), the copolymer with 6.7% of grafted poly(BPOCPA) and the coproducts including 26.7% poly(BPOCPA)

that all of the individual IR bands belonging to both neat HDPE and poly(BPOCPMA) macromolecules were detected in the spectra, Fig. 1. This can be seen as an experimental clue (especially in the copolymer sample) illustrating that the graft copolymerization of BPOCPMA onto HDPE took placed. Furthermore, it was deduced from the figure that the increasing of poly(BPOCPMA) content in the coproduct sample gave rise to that the characteristic absorption bands of poly(BPOCPMA) became more apparent in the spectrum as expected.

DSC (thermal behaviors and crystallinity) and XRD characterization

The effect of the graft copolymerization of BPOCPMA onto HDPE on the thermal behavior of the products was

investigated by DSC. Any endotherm attributable to the crystalline melting of poly(BPOCPMA) component was not detected in any of the thermograms of the products although the homopolymer poly(BPOCPMA) was reported to melt at 121 °C [42]. On the other hand, significant and comparable increases were recorded in the melting temperature of HDPE component in both copolymers and coproducts, Fig. 2. The melting temperatures, however, were more consistent with the poly(BPOCPMA) content in the copolymers, while more scattering and irregular melting points were seen in the coproducts, that is, when the products contained the poly(BPOCPMA) homopolymer macromolecules. The maximum points, 134.1 °C and 134.5 °C were detected in both classes with similar contents, at 11.8% poly(BPOCPMA) in the copolymers and at 12.7% content in the coproducts, respectively. The melting temperatures then tended to decrease as the percentage of poly(BPOCPMA) increased further, and reduced to the values even lower than that of virgin HDPE. In order to reveal the effect of the graft copolymerization on the thermal behavior of the material, a pure HDPE sample and a mixture of HDPE and DCP (2% with respect to weight of HDPE) were annealed at 140 °C for 1 h in vacuum, as in graft copolymerization experiments. The melting temperature of both samples was observed to remain almost unchanged at about 131 °C (the same as virgin HDPE).

The percentage crystallinities (X_c) of the products were calculated by using the formula,

Table 2 The crystallinity of HDPE component in the products

Copolymers		Coproducts	
% poly(BPOCPMA)	X_c (%)	% poly(BPOCPMA)	X_c (%)
3.8	46.4 ± 2.3	3.8	66.1 ± 2.3
6.7	49.0 ± 4.2	7.3	49.4 ± 3.2
10.7	43.8 ± 1.9	12.7	49.5 ± 4.6
11.8	45.6 ± 0.2	19.2	59.6 ± 3.5
18.6	44.8 ± 2.1	25.1	57.0 ± 2.3
21.0	55.7 ± 3.2	26.7	47.8 ± 2.7
Pure HDPE	70.0 ± 3.8		

$$X_c(\%) = \frac{\Delta H_f}{\Delta_{Hf}} \times 100 \quad (1)$$

In the equation; ΔH_f is the heat of fusion, and were obtained from the melting endotherms of the products. ΔH_f is the heat of fusion of 100% crystalline HDPE (293 J/g) [44]. The results were presented in Table 2. The analysis showed that the graft copolymerization led to decreases in the crystallinities the products. The minimum crystallinities were recorded as 43.8% at 10.7% poly(BPOCPMA) in the copolymers and as 47.8% at 26.7 poly(BPOCPMA) in the coproducts while the crystallinity percentage of pure HDPE used in the experiments was 70%. But, it is difficult to express a remarkable trend in the crystallinity behaviors. It can be concluded that the grafted poly(BPOCPMA) macromolecules hindered the

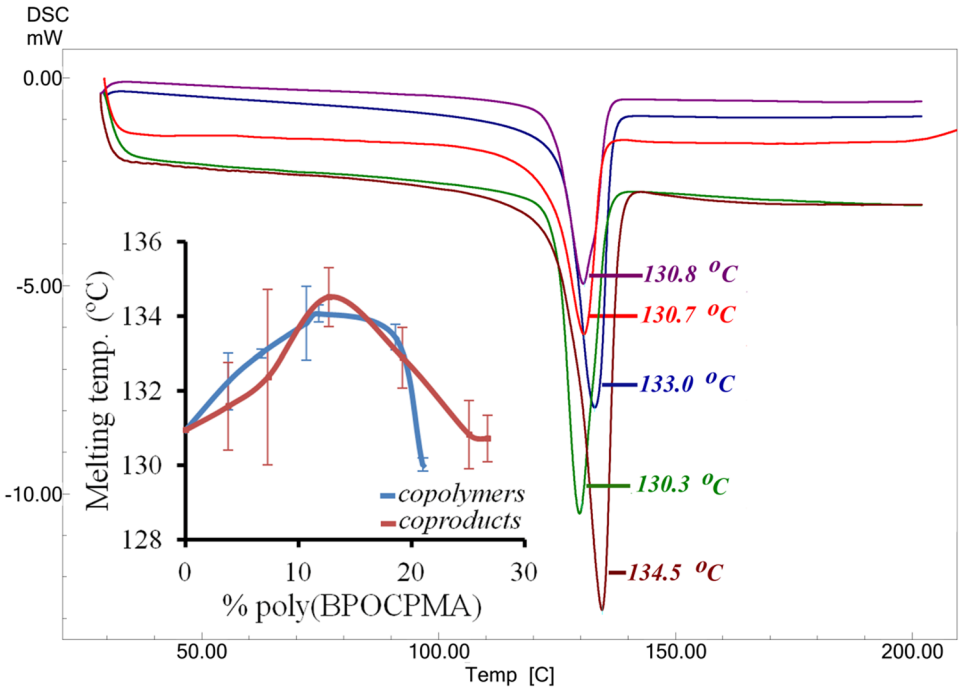

Fig. 2 The DSC thermograms, of HDPE processed with 2% DCP (130.7 °C), of the copolymers with 6.7% poly(BPOCPMA) (133.0 °C), 21% poly(BPOCPMA) (130.3 °C) and of the coproducts with 12.7% poly(BPOCPMA) (134.5 °C), 25.1% poly(BPOCPMA) (130.8 °C), and the variation of HDPE melting temperature with poly(BPOCPMA) content in the products (on the left)

arrangement and packing of HDPE chains in the crystalline order, and thus led to the decreases in the crystallinities.

In order to clarify the effect of the graft copolymerization on the crystalline characteristics of the HDPE, in conjunction with the thermal behaviors, the products were also analyzed by XRD. The crystal parameters were calculated on the basis of a least square method using (hkl) planes and d values. The orthorhombic unit cell size of crystalline domains of the products was estimated from the XRD patterns by using the formula;

$$d = 0.941\lambda/Bcos\theta_B \quad (2)$$

where d is the crystal thickness, λ denotes the wavelength of the XRD source, B is the full width at half maximum (FWHM) of the Bragg peak, and θ_B is the Bragg angle. Here, B is defined as;

$$B^2 = Bm^2 - Bs^2 \quad (3)$$

where, B_s shows the half width of the standard material and B_m is the sign of the difference between the angles at FWHM of the peak.

The XRD analysis showed that the orthorhombic structure in crystalline domains of HDPE matrix has been conserved throughout the graft copolymerizations. This was revealed by the patterns typical of orthorhombic polyethylenes, indicating the crystalline packing of HDPE chains merely in orthorhombic unit cell, Fig. 3. The lateral dimensions of the unit cell, however, were found to be remarkably affected by poly(BPOCPMA) content. Significant increases in the unit cell parameters were observed in both classes of the products.

The variations of the orthorhombic unit cell lateral dimensions, namely the unit cell parameters and the ***ab*** basal area, with poly(BPOCPMA) content in the products were given in Fig. 4. In the copolymers the increases in the parameter *a* were expressively stepwise, Fig. 4a. About 0.27% increase was seen with the graft content in the range of 3.8–10.7% poly(BPOCPMA), while the expansions were observed to be twice of the former increase, about 0.54% in the range 11.8–21.0%. The parameter *b*, on the other hand, without showing any change remained identical to the value of virgin HDPE at low graft percentages, 3.8–10.7%, and then displayed an 0.20% enlargement throughout the contents of 11.8–21.0% poly(BPOCPMA), Fig. 4b. The expansions in the unit cell dimensions were also evidently revealed by the shifts of the reflections toward left in the patterns, Fig. 3. The HDPE chains in the unit cells were probably forced apart laterally by the polar grafted macromolecules, thus giving rise to expansions in the lateral dimensions. Seemingly, this effect was more prominent in the parameter *a*. Similar arguments were reported for the expanded unit cells of oriented and branched polyethylene, in relation to the type, distribution and content of the branches [45–47]. In these papers, the expansions were explained on the basis of the included branches in the crystalline regions compelling the chains to laterally enlarged unit cell dimensions. Additionally, the possibility of branch rejection was also reported for the structural changes [47]. Apparently, at low percentages of about 3.8% poly(BPOCPMA), the graft macromolecules were effective enough to lead to 0.27% increase in the parameter *a* by a force exerted laterally on the HDPE chains. However, further increases in the graft chains up to 10.7% did not give rise to additional expansion,

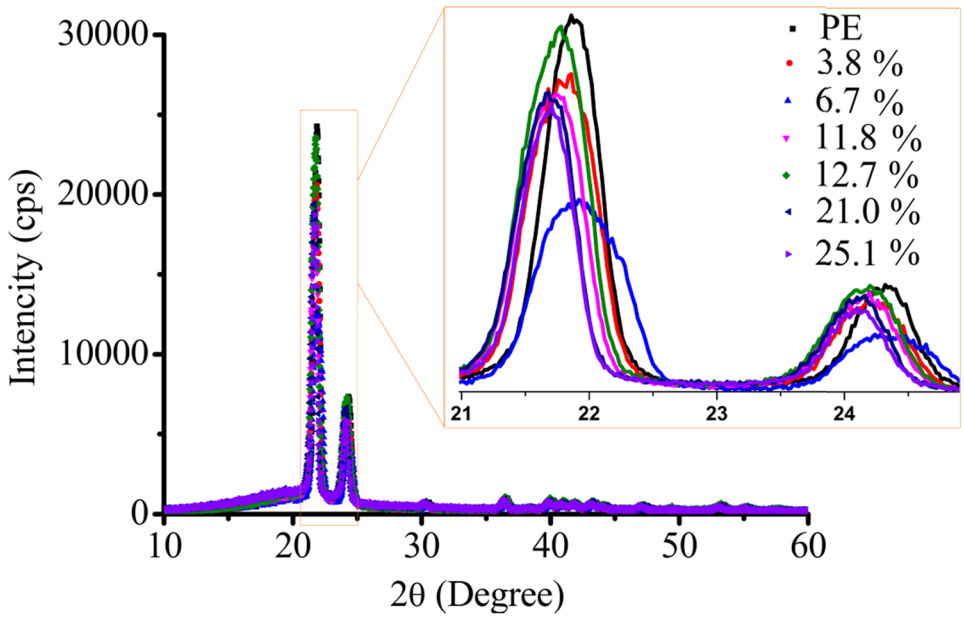

Fig. 3 The XRD patterns of the copolymers involving 6.7, 11.8 and 21.0% poly(BPOCPMA) and of the coproducts involving 3.8, 12.7, 25.1% poly(BPOCPMA)

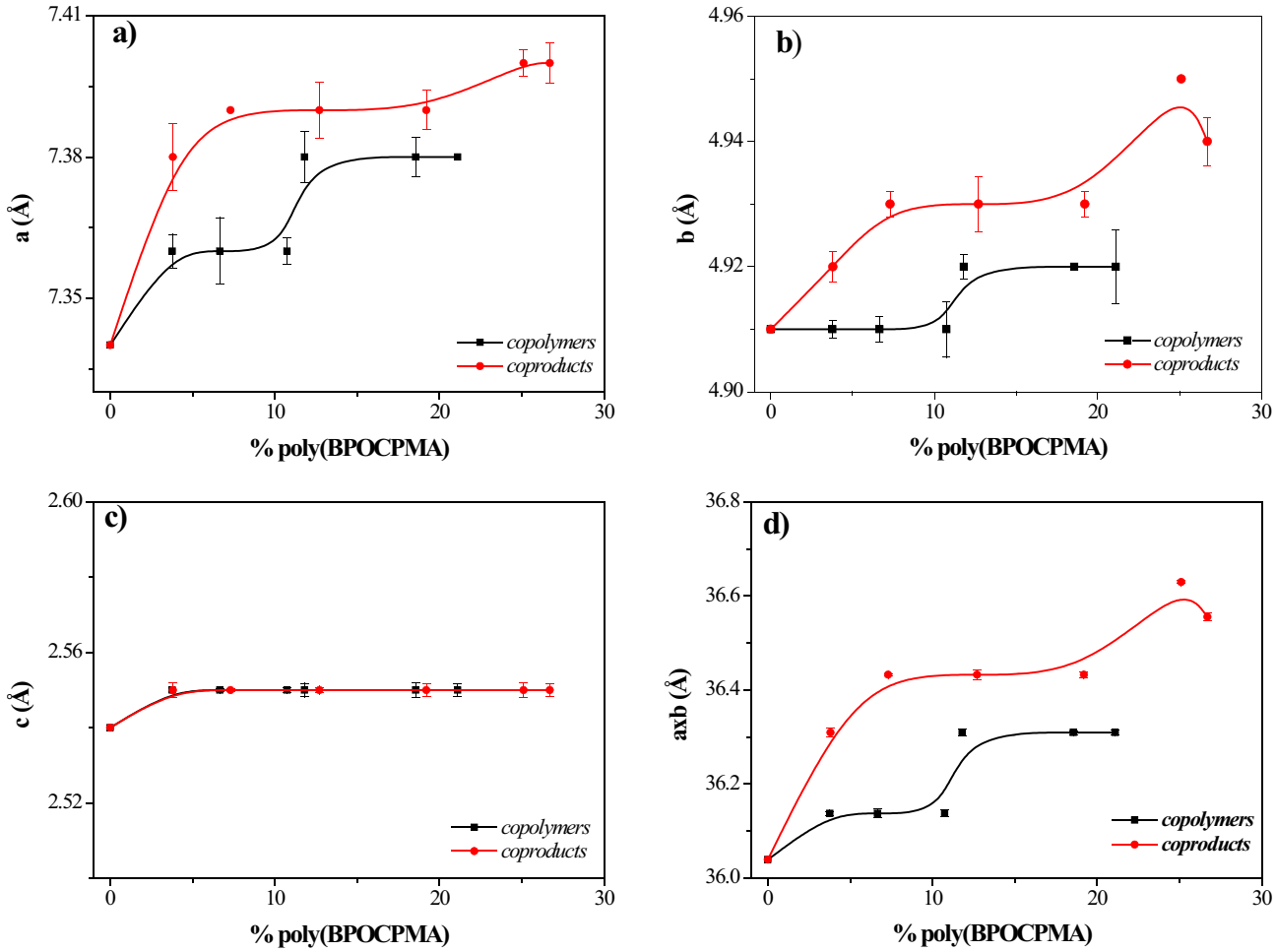

Fig. 4 The variations of the unit cell parameters *a* **a**), *b* **b**) and *c* **c**), and the unit cell basal area *ab* **d**) with poly(BPOCPMA) content, calculated from the X-ray diffraction patterns (using the reflections (110), (200) and (211))

and the parameter *a* remained almost unchanged. Additional increases in poly(BPOCPMA) content from 10.7% up to 21.0% have resulted in another 0.27% enlargement, hence in 0.54% expansion overall. The spatial arrangement and orientation of the graft macromolecules in the products and their relative effects in coercing the HDPE chains apart laterally are believed to resulted in the dissimilar enlargement behaviors in the parameters, and the stepwise behavior was observed in the former parameter. On the other hand, the *c* parameter, i.e., the unit cell axis parallel with the chain axis of HDPE [48] was found to be increased about 0.39% identically in all products, Fig. 4c. The lateral expansions in *a* and *b* dimensions and the corresponding widenings in the *ab* basal area, Fig. 4d, have presumably resulted in the identical enlargements in the *c* axis.

Larger expansions in the *a* and *b* unit cell dimensions and the related wider ***ab*** basal areas were observed in the coproducts which contain poly(BPOCPMA) homopolymer macromolecules as well as the grafted poly(BPOCPMA) chains. The variation of the parameters and the basal area with content of poly(BPOCPMA) were also depicted in Fig. 4. The parameter a increased initially with poly(BPOCPMA) content and reached a plateau value almost 0.68% greater than that of virgin HDPE, at which it remained almost constant along with the percentages 7.3–19.2%. The parameter then increased further to a size 0.81% greater in the 25.1–26.7% poly(BPOCPMA) region, Fig. 4a. A similar trend was also observed in the b parameter which stayed almost constant at the level with 0.41% extension throughout the percentages of 7.3–19.2%. This plateau was then followed by further expansion as the content of poly(BPOCPMA) increased more, and about 0.81% expanded *b* parameter was observed at 25.1% poly(BPOCPMA), Fig. 4b. These results, the greater enlargements in lateral dimensions of the unit cell with the inclusion of the poly(BPOCPMA) homopolymer chains in the coproducts could be explained by the strong interactions between the polar groups of grafted and ungrafted poly(BPOCPMA) homopolymer macromolecules. The

adhesive forces between the polar groups of the grafted and the homopolymer chains have presumably brought about an additional effect in the enlargements of the lateral dimensions. On the other hand, similar to the copolymers, the same expansion, 0.39%, was recorded in the parameter c in all the coproducts, Fig. 4c. The additional increases in the lateral dimensions had no additional effect on the enlargements in the c axis of the unit cells, parallel with the axis of HDPE chains.

The consistent rises in the melting temperature of HDPE as the percentage of poly(BPOCPMA) increased up to about 12% in both classes of the products (Fig. 2) are probably due to the developments in the ordering and orientation of HDPE chains resulting from the grafted side chain LCP poly(BPOCPMA) chains. The poly(BPOCPMA) chains with mesogenic side groups were reported to exhibit glassy nematic arrangement [42]. The grafted poly(BPOCPMA) chains which have the ability/potential of forming reported regularly organized structure probably enhanced the ordering and orientation of HDPE chains during crystallization. Furthermore, the glassy nematic structured poly(BPOCPMA) chains might have acted also as nucleating agents, and thus led to more ordered arrangement and packing of the chains in the crystalline regions. Because, a better array and a promoted arrangement can be potentially expected in the crystal when it originates from a center with more ordered structure. Moreover, a greater conformational freedom arising from the enlargements in the *ab* basal area of the unit cells might have additionally contributed to the promoted ordering and arrangement of the HDPE chains. These probable developments in the microstructure of the material thus may have led to the increased melting temperatures from 131 °C to 134 °C achieved with approximately 12% poly(BPOCPMA) in both classes of the products. On the other hand, the tendency to decrease in the melting point as the poly(BPOCPMA) content increased further was probably due to the relative loss in the promoted arrangement of the chains. That is, the graft chains at percentages higher than 12–13% might have started to lose their assisting function in the ordered and oriented packing of the HDPE chains, probably owing to large space occupations by the poly(BPOCPMA) macromolecules between the chains and to relatively strong interactions between the polar groups of the graft chains. This effect probably became more operative and pronounced with increasing content, and the decrease trends were observed in the melting temperatures after the maximum values.

As for change in the crystal size (grain size) of the products with the percantage of poly(BPOCPMA), it was visible from Fig. 5 that the species showed the similar trends with ab basal area. Namely, crystal size increased initially with the content in both classes of the products. The initial increases were then followed by plateau values. 41–43% and 30% of expansion were recorded in the

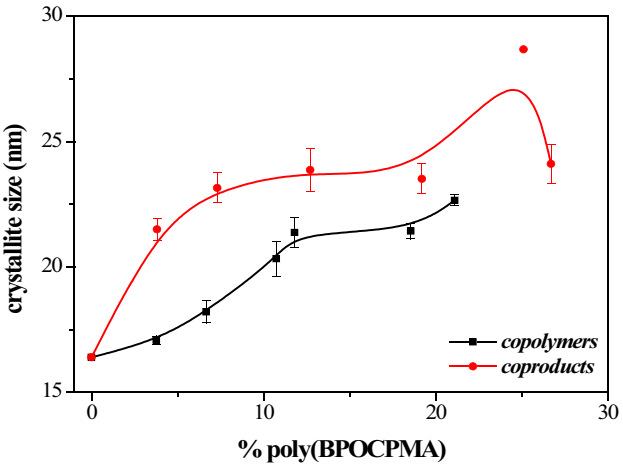

Fig. 5 The variations in the crystal size (grain size) of the products with poly(BPOCPMA) content

coproducts containing 7.3–19.2% poly(BPOCPMA) and in the copolymers with about 11.8–18.6% poly(BPOCPMA, respectively. The sizes continued to rise as the percentage of poly(BPOCPMA) increased further. In the coproducts a maximum size, 28.67 nm (74.8% growth) was recorded at 25.1% of poly(BPOCPMA). The size then exhibited a decline as the content increased more. The similarity observed between the poly(BPOCPMA) content dependence of the ab basal area and the particle size revealed that as the basal area of the unit cells got enlarged, the size of the crystals increased. This behavior could be explained by growth of the crystal to larger size over the large unit cell basal area. That is, the enlargements in the lateral dimensions of the unit cells have seemingly resulted in the extended growth of the crystals to the larger sizes. Moreover, the glassy nematic structured poly(BPOCPMA) chains acting as nucleating agents might have additionally contributed to the promoted growth of the crystals during crystallizations. Because, the crystals can potentially be expected to propagate to larger sizes when they originate from more ordered structures.

PALS analysis of the products

The HDPE used in the experiments and the products were also analyzed by Positron Annihilation Lifetime Spectroscopy in order to investigate their free volume properties. The lifetimes of the positrons for the samples were measured, and the lifetime spectra were deconvoluted into three lifetime components. The shortest-lived component, T_1 with an intensity I_1, the intermediate-lived component, T_2 with an intensity I_2 and the longest-lived component τ_3 with an intensity I_3, were obtained from the spectra. These parameters were calculated using T_1 fixed at 125 ps, assumed as independent of free volume.

In the free volume model, the longest-live component τ_3 is correlated to the free volume hole radius, R whilst I_3 is correlated to the number of holes. That is, an increase in τ_3 value shows an enlargement in the volume of hole, while a rise in I_3 displays an increase in the number of the holes [49].

The radius R (of free volume) was calculated by the semi-empirical approximation given by Eldrup et al. [50] and using *o-Ps* lifetime (τ_3) with the assumption of the holes being spherical;

$$\tau_3(ns) = \frac{1}{2}\left(1 - \frac{R}{R_0} + \frac{1}{2\pi} sin\frac{2\pi R}{R_0}\right)^{-1} \quad (4)$$

where $R_0 = R + \delta R$ with $\delta R = 0.1656$ nm, the thickness of the homogeneous electron layer that constitutes the wall of the hole [51]. The free volume hole size (V_f) was calculated by

$$V_f = \frac{4}{3}\pi R^3 \quad (5)$$

and the free volume fraction (f) proposed by Kobayashi et al. [52] was stated as

$$f_v = AI_3V_f(\tau_3) \quad (6)$$

where A is a proportionality coefficient; that is taken as 0.0018.

The results of the measurements of the ortho-positronium lifetime and the intensity of the longest-lived component of the positrons, the calculated radii of the free volume hole, the free volume hole sizes and the free volume fractions of the products with poly(BPOCPMA) content were given in Table 3.

The *ortho-positronium* lifetime (τ_3), the longest-lived component and associated with pick off annihilation, is proportional to the free volume size in the materials. The variations in the lifetime and the calculated free volume size with the poly(BPOCPMA) content in the products were presented in Fig. 6a and b, respectively. In general, longer lifetime τ_3 values were observed in the coproducts compared to the copolymers at the corresponding poly(BPOCPMA) compositions, Fig. 6a, showing relatively larger free volumes in the coproducts, Fig. 6b. That is, the presence of poly(BPOCPMA) homopolymer chains led to larger free holes in the amorphous region of the coproducts throughout the poly(BPOCPMA) compositions. Seemingly, the ungrafted poly(BPOCPMA) macromolecules played a preventing role from compact packing of the chains in the matrix of the coproducts. Internally, the lifetime τ_3 initially increased at low poly(BPOCPMA) percentages in the coproducts, Fig. 6a. 2.33 ± 0.01 ns (2.2% raise) was measured at 3.8% and 7.3% poly(BPOCPMA). This increase in the τ_3 value signifies an about 3.8% enlargement in the free volume with 129.0 ± 0.8 Å^3 value at the corresponding contents, Fig. 6b. The neat HDPE has the hole size of 124.1 ± 0.7 Å^3 at the prevailing conditions. The lifetime τ_3 then reduced to a plateau value of 2.28 ± 0.01 ns, the same as the value observed in unprocessed HDPE, within 12.7%-25.1% poly(BPOCPMA). Thus the coproduct samples with those poly(BPOCPMA) contents have the free volume hole size identical to that of the pure HDPE. A further increase in the content gave rise to further decrease in the lifetime. 2.23 ± 0.01 ns was recorded at 26.7% poly(BPOCPMA), which demonstrates a moreover reduction in the free volume with size 118.8 ± 0.9 Å^3, almost 4.3% smaller with respect to the pure HDPE.

In the copolymers, a slight increase (0.6%) in the$_3$ value with 2.296 ± 0.010 ns was recorded at 3.8% poly(BPOCPMA). This initial increase in the lifetime, representing an expansion of about 1% in the free volume size, was followed by a gradual decreasing trend as the poly(BPOCPMA) percentage increased further, Fig. 6a and

Table 3 The variations in the ortho-positronium lifetime and the intensities of the positrons, the free volume hole radius and size and the free volume fraction with poly(BPOCPMA) content in **a**) the copolymers and **b**) the coproducts

% poly(BPOCPMA)	Neat HDPE	3.8	6.7	10.7	11.8	18.6	21
τ_3(ns)	2.282 ± 0.009	2.296 ± 0.010	2.272 ± 0.010	2.263 ± 0.010	2.239 ± 0.010	2.222 ± 0.010	2.222 ± 0.010
I_3(%)	23.24 ± 0.08	20.79 ± 0.08	20.01 ± 0.08	19.10 ± 0.08	17.68 ± 0.08	16.96 ± 0.07	15.68 ± 0.07
R(Å)	3.094 ± 0.006	3.105 ± 0.006	3.085 ± 0.006	3.078 ± 0.006	3.058 ± 0.007	3.043 ± 0.007	3.043 ± 0.007
$v_\phi(\oplus^3)$	124.1 ± 0.7	125.4 ± 0.7	123.0 ± 0.7	122.2 ± 0.8	119.8 ± 0.8	118.1 ± 0.8	118.1 ± 0.8
f_v(%)	5.19 ± 0.04	4.69 ± 0.05	4.43 ± 0.04	4.20 ± 0.04	3.81 ± 0.04	3.61 ± 0.04	3.33 ± 0.04
% poly(BPOCPMA)	Neat HDPE	3.8	7.3	12.7	19.2	25.1	26.7
τ_3(ns)	2.28 ± 0.01	2.33 ± 0.01	2.33 ± 0.01	2.28 ± 0.010	2.28 ± 0.010	2.27 ± 0.010	2.23 ± 0.011
I_3(%)	23.24 ± 0.08	20.27 ± 0.08	19.70 ± 0.08	18.79 ± 0.08	18.48 ± 0.07	17.68 ± 0.07	15.11 ± 0.07
R(Å)	3.094 ± 0.006	3.134 ± 0.006	3.133 ± 0.006	3.090 ± 0.007	3.091 ± 0.007	3.086 ± 0.007	3.049 ± 0.007
$v_\phi(\oplus^3)$	124.1 ± 0.7	129.0 ± 0.8	128.8 ± 0.8	123.6 ± 0.8	123.7 ± 0.8	123.0 ± 0.8	118.8 ± 0.9
f_v(%)	5.19 ± 0.04	4.71 ± 0.05	4.57 ± 0.05	4.18 ± 0.04	4.12 ± 0.04	3.92 ± 0.04	3.23 ± 0.04

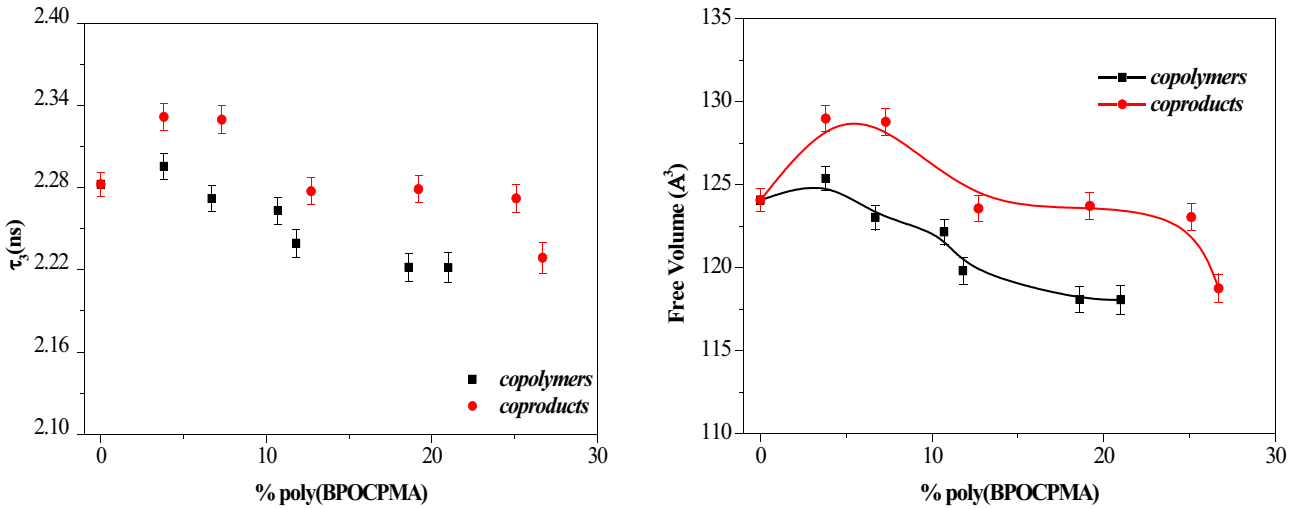

Fig. 6 The variations in **a**) the ortho-positronium lifetime (τ_3), **b**) the free volume size (A^3) with poly(BPOCPMA) content in the products

b. The lifetime 2.222 ± 0.010 ns corresponding to 118.1 ± 0.8 $Å^3$ free volume which is approximately 4.8% smaller compared to the unprocessed HDPE was measured within 18.6%—21.0% poly(BPOCPMA). The initial increase in the free volume size was probably due to larger openings between the chains brought about by the voluminous side groups of the grafted poly(BPOCPMA) that compel the chains laterally and thus prevent close packing. The weak interactions between polar side groups of the grafted macromolecules and the nonpolar HDPE chains might have contributed to the lack of compact packing of the chains. When the poly(BPOCPMA) content exceeds 3.8%, on the other hand, the improved interactions between the chains due to the increased polar group composition probably led to more compact packing of the chains, which resulted in the reduced free volume size in the material. Additionally, the bulky side groups of the grafted poly(BPOCPMA) that give rise to larger openings at low percentages might have largely filled the voids with increased content owing to relatively stronger interactions between the polar groups of the chains.

In the free volume model, the intensity I_3 is proportional to the number of free holes. The I_3 value increases with increasing number of the holes [49]. The variations in the I_3 intensity with poly(BPOCPMA) percentage in the products were plotted in Fig. 7. The intensity decreased as the percentage of poly(BPOCPMA) increased in both the copolymers and the coproducts, more consistently with the content in the former. At low percentages of poly(BPOCPMA) up to about 10%, the downward trend was approximately similar in both classes of the products. At higher contents, however, the intensity was relatively higher in the coproducts comparing to the copolymers, which indicates the higher number of the free holes. Seemingly, the ungrafted poly(BPOCPMA) macromolecules in the coproducts gave rise to more free volume in the matrix as well as to the larger free volumes, probably by playing a preventing role from compact packing of the chains.

The free volume fractions (f) of the products were calculated using the Eq. 6, proposed by Kobayashi et al. [52], in which the free volume size and the intensity were evaluated together. The variations in the fraction with poly(BPOCPMA) percentage in the products were illustrated in Fig. 8. The similar decreasing trends observed in the intensities were also recorded in the fractions. The grafting, while caused small increases in the size of the free volume at relatively lower percentages of poly(BPOCPMA), Fig. 6b, brought about dramatic decreases in its fraction as the content increased, particularly in the copolymers. The improved interactions between the chains due to the increased polar group composition as the content of poly(BPOCPMA) increased probably gave rise to more compact packing of the chains in the matrix, which led to the decreases in the free volume fraction. The presence of the poly(BPOCPMA) homopolymer macromolecules in the coproducts, however, resulted in smaller decreases in the fraction, presumably

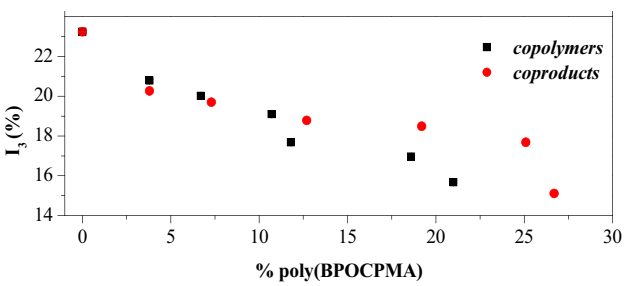

Fig. 7 The variations in the intensity I_3 with poly(BPOCPMA) content in the products

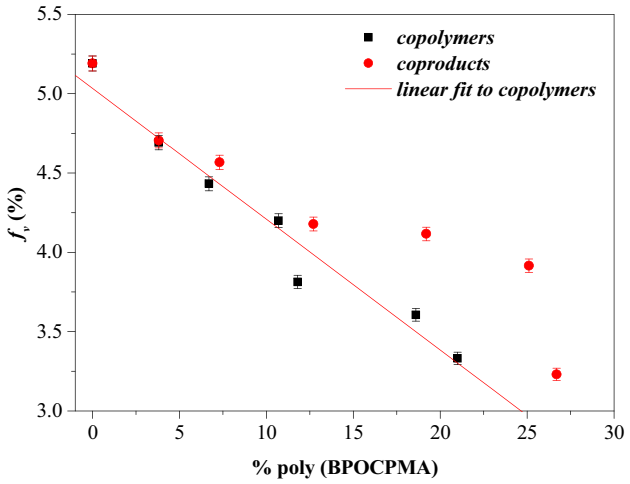

Fig. 8 The variations in the free volume fraction with poly(BPOCPMA) content in the products

by playing a preventing role in the compact packing of the grafted HDPE chains.

Mechanical properties

The function of the graft copolymerization of BPOCPMA on the mechanical behavior of the material has been studied by analyzing the stress–strain and impact behavior of the products. Remarkable improvements were achieved in the mechanical properties of the products, particularly, in ultimate tensile strength and modulus. However, the percent elongation decreased as the poly(BPOCPMA) content increased, and yield stress disappeared at high contents and brittleness prevailed in the mechanical behaviors.

Typical stress–strain curves of neat HDPE and the products were illustrated in Fig. 9. The extensive cold drawing observed in neat HDPE was not recorded in any product, even at low contents of poly(BPOCPMA). As seen in the stress–strain behaviors, Fig. 9, percent elongation decreased as the poly(BPOCPMA) content increased. At low percentages of poly(BPOCPMA), both copolymers and coproducts failed during strain softening and exhibited ductile failure with neck formation. But, longer elongations in the softening, prior to failure, were observed in the coproducts which contain the ungrafted poly(BPOCPMA) macromolecules. The percent elongations were recorded between approximately 15% and 46% in the coproducts while they were observed between about 15% and 34% in the copolymers. That is, the presence of ungrafted, poly(BPOCPMA) macromolecules in the products apparently gave rise to greater flow of HDPE molecules in necking and thus relatively longer elongations in the drawing direction. This statement was evidently supported by SEM analysis in which relatively wider and longer extensions were observed in fractographs of the coproduct samples at the corresponding poly(BPOCPMA) contents, and some small and fine extensions were recorded even at high contents of poly(BPOCPMA) (Sect. 3.5). At relatively high percentages of poly(BPOCPMA), on the other hand, brittle nature started to prevail in the behaviors. The samples involving about 18% poly(BPOCPMA) in the copolymers and 25% poly(BPOCPMA) in the coproducts failed at the beginning of plastic deformation, just before or at the yield point. At higher respective contents, the products then exhibited brittle fracture in the tests. Conclusively, the products revealed a gradual transition from viscoelastic behavior to brittleness in nature with increasing

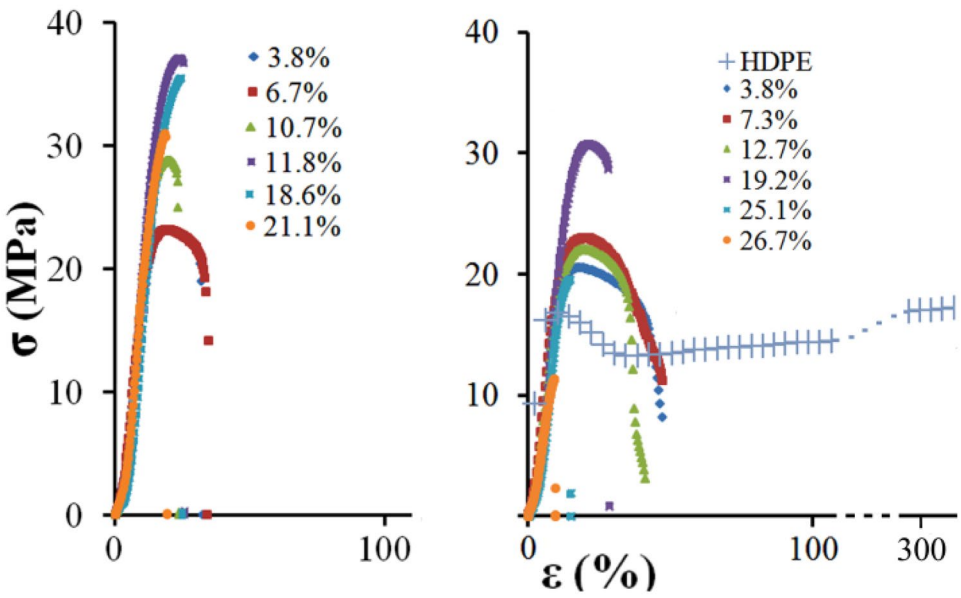

Fig. 9 Stress–strain curves of neat HDPE, the copolymers and the coproducts

poly(BPOCPMA) content. The SEM analysis of the samples also evidently revealed this transition (Sect. 3.5).

The results of the tensile tests of the products, the variations of the tensile strength and Young's modulus with poly(BPOCPMA) content were drawn in Fig. 10a and b, respectively. The tensile strength initially increased with the percentage of poly(BPOCPMA) in both the copolymers and the coproducts, yet in the former the strengths were relatively higher. The maximum strength, 36.3 MPa (93% improvement compared to neat HDPE) was achieved at 11.8% poly(BPOCPMA) in the copolymers. In the coproducts, the maximum of 31.8 MPa (69% improvement) was recorded at 19.2% poly(BPOCPMA). The maxima were then followed by a slow decrease in the former and a relatively drastic decrease in the latter. Almost identical trends were also recorded in Young's modulus, determined on the same samples during the tensile tests. The maxima of 514 MPa (42% rise) and 479 MPa (32% rise) in the modulus were recorded at the same corresponding

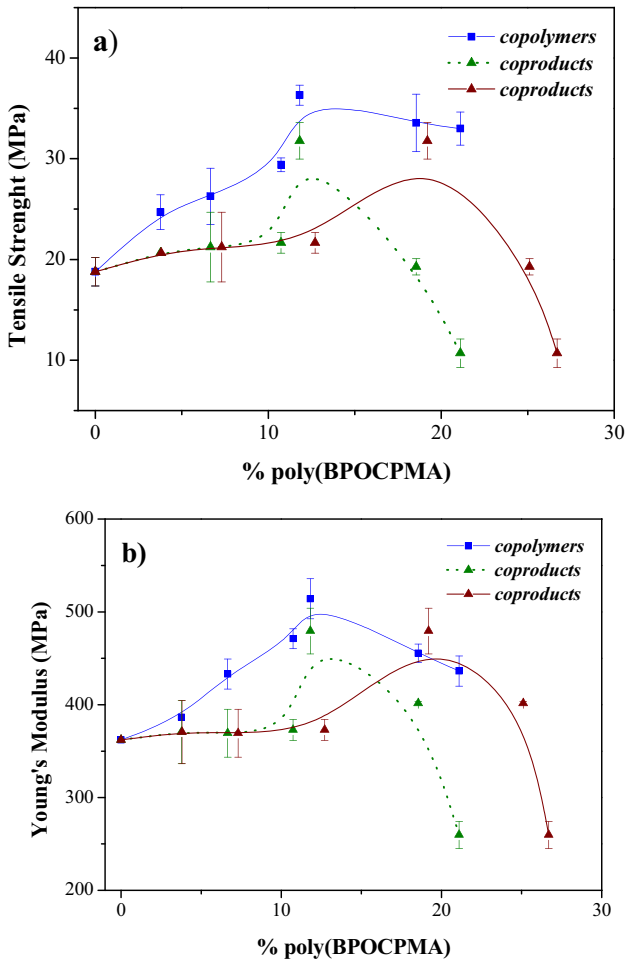

Fig. 10 The variations in **a**) the ultimate strength and **b**) the Young's modulus of the copolymers and the coproducts with poly(BPOCPMA) content

percentages of poly(BPOCPMA) at which the strength maxima were observed, Fig. 10b. These improvements in the tensile behaviors are comparable with those obtained by several main chain LCP reinforcements at similar LCP contents [3, 6]. In fact, the maxima in the tensile properties of both copolymers and coproducts were achieved with approximately the same grafted poly(BPOCPMA) contents. Because, the coproduct containing 19.2% poly(BPOCPMA), at which the maximum strength and modulus were recorded, involves about 12% poly(BPOCPMA) present as grafted chains and about 7% poly(BPOCPMA) present as ungrafted homopolymer macromolecules. The green dotted lines in Fig. 10a and b show the variations drawn with this regard, that is, they were drawn by considering the percentages of grafted poly(BPOCPMA) only, by excluding the ungrafted poly(BPOCPMA) present as homopolymer macromolecules in the coproducts.

The PALS analysis of the products indicated that the mechanical behaviors of the products were significantly governed by their free volume properties. The percent elongation decreased consistently with the decrease of free volume fraction as the percentage of poly(BPOCPMA) increased in the products. The initial improvements in the tensile strength and the modulus with the increase in the content of poly(BPOCPMA) were firmly accompanied by the decreases in the free volume fraction. Especially, it is very striking that the sharp increase in the tensile strength (from 29.4 MPa to 36.30 MPa) and the modulus (from 471 to 514 MPa), when the percentage of poly(BPOCPMA) increased from 10.7% to 11.8% in the copolymers, were accompanied with the sharp decrease in the free volume fraction (from 4.20% to 3.81%).

The chain slip mechanism was reported to be the dominant mode of plastic deformation in the crystalline part of semicrystalline polymers, and it has a major role in the plastic strains [16, 17]. The cavities forming in the material under load were stated to give rise to a local release of stress around the voids [31, 33], triggering of the unravelling of the folded chains and thus breaking down the crystals [34]. Consistently, the formation of voids leads to the fragmentation and fibrillar transformation of the crystalline lamellae beyond yielding [35]. The decrease in the percent elongation and the initial improvements in the tensile properties of the products as the content of poly(BPOCPMA) increased are most likely due to the decrease in the free volume fraction of the material. It seems that the increased stress in the material arising from the decrease in the free volume fraction resulted in a lower chain slip and flow ability in the draw direction and a lower conformational freedom, which have brought about a shorter flow of the chains in the softenings and thus the shorter elongations. In addition, the lower slip and flow ability of the chains and the lower conformational freedom have presumably given rise to the higher tensile strengths and the modulie, that is, to the superior withstanding

behaviors under the load. Furthermore, a better distribution of the tensile load between the chains, which conduce by the more compact packing of the macromolecules together with the decrease in the free volume fraction, might have additionally contributed to the superior tensile behaviors. The longer elongations and the lower tensile strength and modulus characteristics, recorded in the tests, of the coproducts which have relatively larger free volumes and the greater fractions comparing to the copolymers, evidently support the proposed relations between the mechanical behaviors and the free volume properties of the products. On the other hand, the rigid character of poly(BPOCPMA) macromolecules at room temperature (with T_g value of 72 °C [42]), stemming from its voluminous and rigid side groups with polar nature, might have contributed to the restricted mobility and flow of the chains. In the tests, the effect of this contribution on the plastic deformation of the products was probably even more pronounced with the increase of poly(BPOCPMA) content.

Developments in the alignment and orientation of HDPE chains due to the constitution of grafted side chain LCP poly(BPOCPMA) macromolecules might have also played role in the improvements of the tensile behaviors. That is, the potential of forming glassy nematic arrangement of poly(BPOCPMA) chains [42] may have conduced to a promoted ordering and orientation of HDPE chains in the products. These developments might have contributed to the advanced tensile behaviors as well to the increased melting temperatures of crystalline domains in the HDPE matrix. In addition, it is noteworthy the microstructural changes, namely, the expansions in the unit cell dimensions of the orthorhombic structure for the resulting improvements. The initial increase trends in the tensile behaviors and the melting temperature were accompanied by the increases in the *a* and *b* unit cell parameters. Conveniently, the higher conformational freedom of the chains owing to the larger *ab* basal area might have cooperated with cohesive forces of the polar grafted macromolecules and played a role in conducing to improved arrangement of the HDPE chains. These developments thus might have made a contribution to the achievement of the resulting improvements in the tensile behaviors.

The presence of the poly(BPOCPMA) homopolymer macromolecules in the coproducts, on the other hand, led to relatively lower improvements in the tensile behaviors, and caused the coproducts to exhibit relatively sharp decreases after the maxima in the tensile strength and the modulus, Fig. 10a and b. The PALS analysis showed that the coproducts had larger free volumes and generally larger free volume fractions compared to the copolymers. Apparently, the poly(BPOCPMA) homopolymer macromolecules played a role in preventing the chains in the matrix from packing in a compact way. Relatively lower stress and higher conformational freedom, owing to the larger free volume and the larger free volume fraction, presumably resulted in higher slip and flow ability of the chains. The higher slip and flow ability of chains in the coproducts likely led to the longer elongations in the tensile tests and the relatively lower improvements in the tensile strengths and the moduli, that is, to relatively lower withstanding characteristics under tensile load. Further, relatively lower tensile load distribution between the chains due to the relatively loose packing, together with the larger free volume and the larger free volume fraction, may have also contributed to the lower improvements in the tensile properties of the coproducts. Moreover, the greater expansions of a and b unit cell dimensions and the corresponding enlargements in the ab basal area were observed in the coproducts relative to the copolymers, as discussed in the XRD characterizations. The higher conformational freedom in the larger ab basal area might have played a role in relatively easier unravelling of folded chains and fragmentation of the crystals and hence in the longer elongations. In addition, the relatively easier unravelling of the folded chains might have resulted in the relatively lower withstanding behaviors under tensile load, that is, in the relatively lower tensile characteristics. Furthermore, low tensile load capacity of homopolymer poly(BPOCPMA) chains might have contributed to the relatively lower improvements in the tensile behaviors. Because, it is unlikely that a polymer consisting of chains with so bulky and rigid side groups will exhibit significant strength under the load relative to HDPE. Hence, the presence of poly(BPOCPMA) homopolymer chains may have made the coproducts less prone to resist in the tensile tests, which was more pronounced at high contents.

The impact behavior of the products was investigated by Izod impact test. In spite of the brittleness observed in the tensile tests, particularly at high contents of poly(BPOCPMA), almost all the samples were not

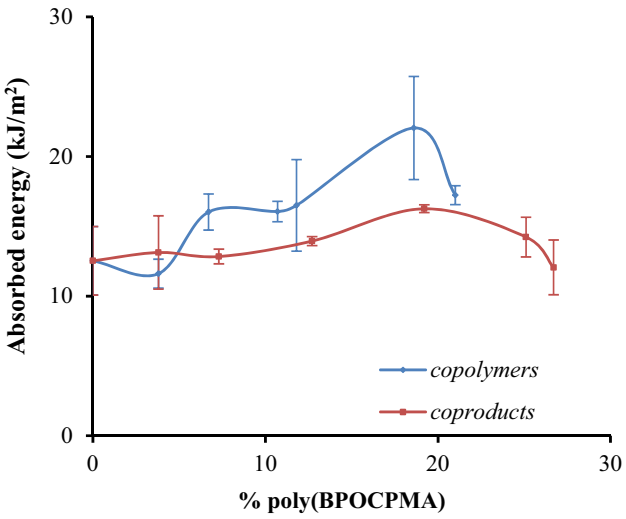

Fig. 11 The variations of the absorbed energy with poly(BPOCPMA) content in the products in the impact tests

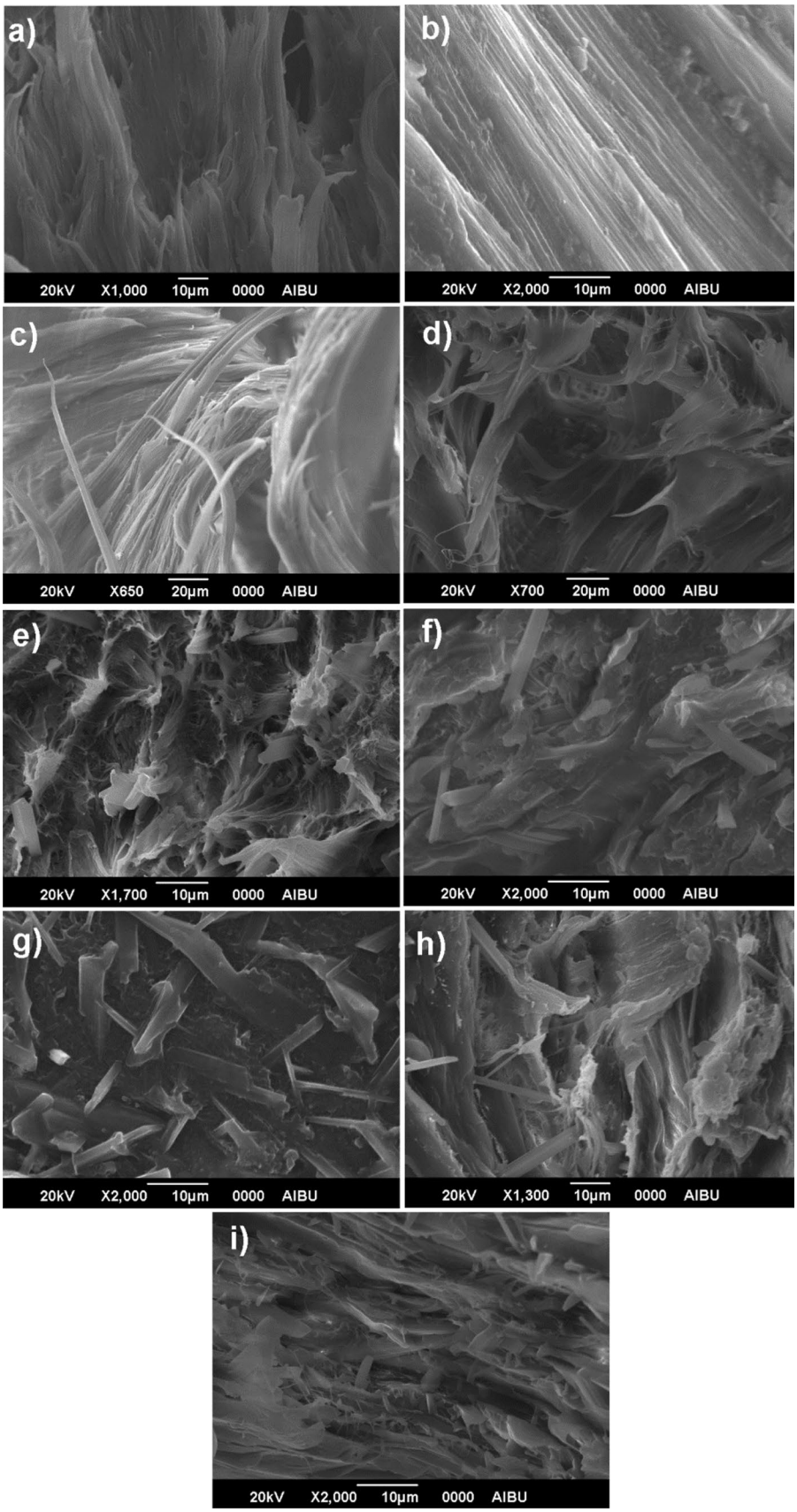

Fig. 12 SEM micrographs of the tensile fractured surfaces of **a)** the coproduct with 3.8%, **b)** the copolymer with 6.7%, **c**) the copolymer with 10.7%, **d)** the coproduct with 12.7%, **e)** the coproduct with 25.1%, **f)** the copolymer with 18.6%, **g)** the copolymer with 21.0%, **h)** the coproduct with 26.7% poly(BPOCPMA) and **i)** the impact fractured surface of the coproduct with 26.7% poly(BPOCPMA)

broken in the impact tests, except for the coproduct involving 26.7% poly(BPOCPMA) which exhibited an impact strength of 12.06 kJ/m^2. On the other hand, it was observed that the energy absorbed by nonbroken samples gradually increased as the poly(BPOCPMA) content in the copolymers increased, Fig. 11. The energy reached the maximum 22 kJm^{-2} (76% increase compared to HDPE) at 18.6% poly(BPOCPMA) and then decreased sharply with a further increase in the content. A very slight increase trend in the energy absorbed was also observed in the coproducts. It seems that the energy (absorbed by nonbroken samples) in the impact tests increased as the products became more compact. As revealed by the PALS analysis, the free volume fraction decreased and thus the products became more compact as the content of poly(BPOCPMA) increased. The increase of compactness in the structure resulted in the absorption of more energy loaded in the impact tests. The greater absorbed energy and the smaller free volume properties of the copolymers, comparing to the coproducts, evidently support the proposed relation between the absorbed energy and the free volume characteristics of the products. On the other hand, the possible improvements in the alignment and orientation of HDPE chains due to the constitution of the side chain LCP poly(BPOCPMA) macromolecules might also have contributed to the advances in the absorption of the energies recorded in the tests. This argument was supported by the extensive fibrillar structure with ductile extensions at low percentages of poly(BPOCPMA) and the existence of small and thin fibrils even at high contents of poly(BPOCPMA), as revealed in the impact fractographs, Fig. 12. Nevertheless, poly(BPOCPMA) can be expected to exhibit a lower resistance to break due to the chains with the voluminous and rigid side groups and hence with a relatively high T_g value (72 °C [42]), and thus can be predicted to impart brittleness to the products.

SEM analysis of the products

Size, size distribution of reinforcement phase and the adhesion quality of interface between matrix and the reinforcement phase are important factors for the mechanical performance of polymer blends and composites. Therefore, the tensile and impact fractured surfaces of the products were investigated by SEM analysis. The SEM micrographs, Fig. 12, revealed that the products exhibited no phase separation, and their structures were completely homogeneous although the graft poly(BPOCPMA) chains with polar side groups are essentially different in nature from apolar HDPE. This morphological behavior of the products confirmed the chemical bonding of the poly(BPOCPMA) macromolecules, that is, the graft copolymerization of BPOCPMA onto HDPE. Moreover, the homogeneous structure of the products demonstrated that the HDPE-g-poly(BPOCPMA) macromolecules acted as compatibilizer providing good interfacial adhesion between the poly(BPOCPMA) homopolymer macromolecules and the HDPE matrix in the coproducts.

The analysis of the products displayed a gradual transition from ductile fracture at lower poly(BPOCPMA) contents to brittle nature dominated at high percentages. The bulky and long extensions like fibrillar structure observed at lower percentages gradually got smaller and shortened as the content increased. (Fig. 12a-e). On the other hand, it can be stated as a general deduction that the copolymers exhibited better fibrillations and orientations at similar contents of poly(BPOCPMA), comparing to the coproducts, as revealed by the oriented structures (Fig. 12b and c) and thin extensions from the surfaces, widely observed in the copolymer samples (Fig. 11f and g). Accordingly, the better alignment and orientation in the fibrillar structure additionally account for the better improvements in the mechanical behavior of the copolymers. At high percentages of poly(BPOCPMA) the gradually shortened extensions were eventually replaced by a morphology revealing brittle fracture in majority, verified by the cracks and openings on the surfaces. But, the transition took place at earlier percentages in the copolymers, confirmed by the existence of small extensions even at high contents in the coproducts (Fig. 12e and h). This is also consistent with the more compact structure of the copolymers. That is, the lower conformational freedom of the chains in the more compact structure with the lower free volume fraction probably caused the copolymers to exhibit brittle fracture at relatively earlier percentages of poly(BPOCPMA). On the other hand, there still existed some fibrillar extensions even at high contents of poly(BPOCPMA). These extensions were observed in the fractographs as thin fibrils protruding from the surfaces broken in brittle nature in the copolymer samples, and as small extensions in some coproduct samples (Fig. 12f–h). The thin fibrils were also seen in the impact fractograph of the coproduct sample involving 26.7% poly(BPOCPMA), besides the cracks and openings showing the brittle fracture (Fig. 12i). But, the materials did not show any phase separation at all.

Conclusion

- The graft copolymerization resulted in significant increases in the unit cell dimensions, *a* and *b* parameters, of the orthorhombic structure of HDPE, in consistence with the content of poly(BPOCPMA). The grafted poly(BPOCPMA) macromolecules with rigid, large and polar side groups probably forced the HDPE chains apart laterally and thus expanded the unit cell dimensions. A constant expansion in the parameter *c*, however,

was recorded in all products. Furthermore, a similar increase trend was also observed in the crystal size in crystalline domains of HDPE matrix with the content of poly(BPOCPMA).

• At relatively lower percentages, the poly(BPOCPMA) macromolecules with the voluminous side groups probably compelled the HDPE chains laterally, prevented close packing and thus resulted in the increases in the free volume size. As the content of poly(BPOCPMA) increased, the improving interactions between the chains due to the increased polar group composition most likely brought about more compact packing of the chains, and thus led to the smaller free volumes in the products and to the decreases in the free volume fraction. The presence of the poly(BPOCPMA) homopolymer macromolecules, however, resulted in smaller decrease in the free volume fraction, presumably by playing a role in preventing packing of the grafted HDPE chains in a compact way in the coproducts.

• The graft copolymerization resulted in the remarkable improvements in the mechanical properties of the products, especially, in the ultimate tensile strength and the modulus. Brittleness dominated in the mechanical behaviors at high contents of poly(BPOCPMA).

• The mechanical behaviors of the products were significantly governed by their free volume properties. The loss in the percent elongation and the initial improvements in the tensile properties of the products as the content of poly(BPOCPMA) increased are probably due to the decrease in the free volume fraction of the products. The probable increase in the stress in the products arising from the decrease in the free volume fraction, resulting in a lower chain slip and flow ability in the draw direction and a lower conformational freedom, have presumably brought about shorter flow of the chains in the softenings and thus in the shorter elongations, and given rise to the higher tensile strengths and the modulie. A better distribution of the tensile load between the chains, conduced by the more compact packing of the macromolecules together with the decrease in the free volume fraction, might have additionally contributed to the superior tensile behaviors.

• The presence of the poly(BPOCPMA) homopolymer chains in the coproducts led to relatively lower improvements in the tensile behaviors. Probably, relatively lower stress and higher conformational freedom, owing to the larger free volume and the larger free volume fraction, resulted in higher slip and flow ability of the chains and thus led to the longer elongations in the tensile tests and the relatively lower improvements in the tensile strengths and the moduli. Relatively lower tensile load distribution between the chains due to the relatively loose packing, together with the larger free volume and the larger free volume fraction, may have also contributed to the relatively lower improvements in the tensile properties of the coproducts.

• The structures of all the products were homogeneous. The products exhibited a gradual transition from viscoelastic behavior prevailed at lower contents of poly(BPOCPMA) to brittle nature dominated at high percentages.

Supplementary Information The online version contains supplementary material available at https://doi.org/10.1007/s10965-021-02646-3.

Acknowledgements This work was supported by BAIBU research fund grant no. BAP-2010.03.03.372. The authors thank to Prof. Dr. T. Tinçer for providing his laboratory for the mechanical tests, Prof. Dr. Ugur Yahşi for PALS analysis, Marmara Positronium Laboratory (MARPOS) in Physics Department at Marmara University, Prof. Dr. A. Varilci for SEM analyses, and YENIGIDAM Research Center for DSC analyses.

References

1. Tan N, Ben Jar PY (2019) Polymers 11:1415
2. Machiels AGC, Denys KFJ, VanDam J, DeBoer AP (1997) Polym Eng Sci 37:59
3. Zhou JS, Yan FY (2004) Polym Test 23:827
4. Postema AR, Fennis PJ (1997) Polymer 38:5557
5. Saengsuwan S, Bualek-Limcharoen S, Mitchell GR, Olley RH (2003) Polymer 44:3407
6. Ivanova T, Zicans J, Elksnite I, Kalnins M, Maksimov R (2011) J Appl Polym Sci 122:3564
7. Odonnell HJ, Baird DG (1995) Polymer 36:3113
8. Tjong SC, Meng Y (1997) Polym Int 42:209
9. Deblieck RAC, Van Beek DJM, Remerie K, Ward IM (2011) Polymer 52:2979
10. Lin X, Caton-Rose F, Ren D, Wang K, Coates P (2013) J Polym Res 20:122
11. Tian Y, Zhua C, Gong J, Yang S, Ma J, J Xu (2014) Polymer 55:4299
12. Yang HR, Lei J, Li L, Fu Q, Li ZM (2012) Macromolecules 45:6600
13. Hossain D, Tschopp MA, Ward DK, Bouvard JL, Wang P, Horstemeyer MF (2010) Polymer 51:6071
14. Kim JM, Locker R, Gregory RC (2014) Macromolecules 47:2515
15. Rozanski A (2018) J Polym Sci Part B Polym Phys 56:1203
16. Butler MF, Donald AM, Ryan AJ (1998) Polymer 39:39
17. Bartczak Z, Vozniak A (2019) Polymers 11:1954
18. Farge L, Boisse J, Dillet J, Andre S, Albouy P-A, Meneau FJ (2015) Polym Sci Part B Polym Phys 53:1470
19. Humbert S, Lame O, Chenal J-M, Seguela R, Vigier G (2012) Eur Polym J 48:1093
20. Humbert S, Lame O, Vigier G (2009) Polymer 50:3755
21. Nilsson F, Lan X, Gkourmpis T, Hedenqvist MS, Gedde UW (2012) Polymer 53:3594
22. Seguela R (2005) J Polym Sci Part B Polym Phys 43:1729
23. Hiss R, Hobeika S, Lynn C, Strobl G (1999) Macromolecules 32:4390
24. Patlazhan S, Remond Y (2012) J Mater Sci 47:6749
25. Pawlak A, Krajenta J, Galeski A (2018) Polymer 151:15
26. Pawlak A, Galeski A (2005) Macromolecules 38:9688

27. Humbert S, Lame O, Chenal JM, Rochas C, Vigier G (2010) Macromolecules 43:7212
28. Pawlak A, Galeski A, Rozanski A (2014) Prog Polym Sci 39:921
29. Chen R, Lu Y, Jiang Z, Men Y (2018) J Phys Chem B 122:4159
30. Pawlak A (2007) Polymer 48:1397
31. Pawlak A, Galeski A (2008) Macromolecules 41:2839
32. Deburck SCY (2007) Mater Sci Eng A 448:56
33. Galeski A (2003) Prog Polym Sci 28:1643
34. Galeski A, Bartczak Z (2010) Macromol Symp 294-I:67
35. Xiong B, Lame O, Chenal JM, Rochas C, Seguela R, Vigier G (2013) Polymer 54:5408
36. Sharma SK, Pujari PK (2017) Prog Polym Sci 75:31
37. Ponnamma D, Ramachandran R, Hussain S, Rajaraman R, Amarendra G, Varughese KT, Thomas S (2015) Comp Part A Appl Sci Manufact 77:164
38. Yu RS, Suzuki T, Djourelov N, Ito Y, Kondo K (2006) Rad Phys Chem 75:247
39. Djourelov N, He C, Suzuki T, Shantarovich VP, Ito Y, Kondo K, Ito Y (2003) Rad Phys Chem 68:689
40. Dai YQ, Wang B, Wang SJ, Jiang T, Cheng SY (2003) Rad Phys Chem 68:493
41. Terlemezyan L, Mokreva P, Tsocheva D, Peneva S, Berovsky K, Troev T (2008) Rad Phys Chem 77:591
42. Sainath AVS, Rao AK, Reddy AVR (2000) J Appl Polym Sci 75:465
43. Kirkegaard P, Eldrup M, Mogensen OE, Pedersen NJ (1981) Comp Phys Commun 23:307
44. Weon JI (2010) Polym Degrad Stabil 95:14
45. Howard PR, Crist B (1989) J Polym Sci Pol Phys 27:2269
46. Baker AME, Windle AH (2001) Polymer 42:651
47. Baker AME, Windle AH (2001) Polymer 42:681
48. Peacock A (2000) Handbook of Polyethylene, Marcel Dekker Inc New York
49. Mostafa N, Ali EH, Mohsen M (2009) J Appl Polym Sci 113:3228
50. Eldrup M, Lightbody D, Sherwood JN (1981) Chem Phys 63:51
51. Nakanishi H, Jean YC (1990) Positron and Positronium Chemistry, Elsevier (Chapter 5), Amsterdam
52. Kobayashi Y, Zheng W, Meyer EF, McGervey JD, Jamieson AM, Simha R (1989) Macromolecules 22:2302